



Original Article

Topoisomerase I Inhibition Radiosensitizing Hepatocellular Carcinoma by RNF144A-mediated DNA-PKcs Ubiquitination and Natural Killer Cell Cytotoxicity

Chiao-Ling Tsai^{1,2}, Po-Sheng Yang³, Feng-Ming Hsu^{2,4}, Ann-Lii Cheng⁵, Wan-Ni Yu⁶ and Jason Chia-Hsien Cheng^{1,2,4*}

¹Graduate Institute of Clinical Medicine, National Taiwan University College of Medicine, Taipei; ²Division of Radiation Oncology, Department of Oncology, National Taiwan University Hospital, Taipei; ³Department of General Surgery, Mackay Memorial Hospital, Taipei; ⁴Graduate Institute of Oncology, National Taiwan University College of Medicine, Taipei; ⁵Cancer Center, National Taiwan University, Taipei; ⁶Taiwan Liposome Company, Taipei

Received: 2 June 2022 | Revised: 8 September 2022 | Accepted: 21 September 2022 | Published online: 4 January 2023

Abstract

Background and Aims: Topoisomerase I (TOP1) participates the repair of DNA double-strand breaks (DSBs) upon radiation therapy (RT). RNF144A mediates ubiquitination of catalytic subunit of DNA protein kinase (DNA-PKcs), a critical factor in DSB repair. This study aimed to investigate the natural killer (NK) cell-mediated radiosensitization with TOP1 inhibition and the mechanism by DNA-PKcs/RNF144A. **Methods:** *In vitro* synergism with TOP1i or cocultured NK cells and RT were evaluated in human hepatocellular carcinoma (HCC) cell lines (Huh7/PLC5) by clonogenic survivals. Orthotopic xenografts were treated with Lipotecan and/or RT. Protein expression was analyzed by western blotting, immunoprecipitation, subcellular fractionation, and confocal microscopy. **Results:** Lipotecan/RT had a superior synergistic effect to RT on HCC cells. Combined RT/Lipotecan reduced the xenograft size by 7-fold than RT ($p < 0.05$). Lipotecan caused more radiation-induced DNA damage and DNA-PKcs signaling. The expression of major histocompatibility complex class I-related chain A and B (MICA/B) on tumor cells is associated with the sensitivity to NK cell-mediated lysis. Cocultured NK and HCC cells with Lipotecan radiosensitized HCC cells/tissues with the expression of MICA/B. RNF144A increased more in Huh7 cells with combined RT/TOP1i, and reduced the pro-survival function of DNA-PKcs. The effect was reversed by inhibiting the ubiquitin/proteasome system. In comparison, RNF144A decreased through nuclear translocation with the cumulated DNA-PKcs and radio-resistance of PLC5 cells. **Conclusions:** TOP1i reinforces NK cell-activated

anti-HCC effect of RT through RNF144A mediated DNA-PKcs ubiquitination. RNF144A provides a reason for differentiating radiosensitization effect between HCC cells.

Citation of this article: Tsai CL, Yang PS, Hsu FM, Cheng AL, Yu WN, Cheng JCH. Topoisomerase I Inhibition Radiosensitizing Hepatocellular Carcinoma by RNF144A-mediated DNA-PKcs Ubiquitination and Natural Killer Cell Cytotoxicity. *J Clin Transl Hepatol* 2023;11(3):614–625. doi: 10.14218/JCTH.2022.00271.

Introduction

Hepatocellular carcinoma (HCC) is one of the most common malignancies worldwide and ranked as the second leading cause of cancer-related death.¹ Due to pre-existing liver cirrhosis, co-morbidities, or poor performance status, most patients with locally advanced HCC are not eligible for potentially curative treatment.² With the advancement of technology, radiotherapy (RT) has become one of the treatment choices for localized HCC tumor(s) not suitable for the conventional treatments.³ However, enhancing the therapeutic effect of RT while protecting the surrounding healthy tissue is a great challenge to liver tumors. Hence, specific compounds targeting the inhibition of radiation-activated signaling might meet the requirement.⁴

Sorafenib, a multikinase inhibitor, provides an additional therapeutic option for HCC patients with extrahepatic spread or vascular invasion, and improves the survival rate among patients with advanced HCC.⁵ Several preclinical studies investigated the radiosensitizing effect of sorafenib *in vitro* and *in vivo*.⁶ Combination of RT and sorafenib in unresectable HCC showed toxicities in phase I and II clinical trials.⁷

The lethal effect of RT on cancer cells is the DNA double-strand break (DSB). Type I topoisomerase (TOP1) is the key enzyme involved in DNA DSB repair.⁸ Inhibition of topoisomerases causes DNA damage, inhibits DNA replication, fails to repair strand breaks and results in cell death. Classic example of TOP1 inhibitors (TOP1i) are camptothecins, including topotecan (Hycamtin), irinotecan (CPT11), and their

Keywords: Hepatocellular carcinoma; Radiotherapy; DNA topoisomerase I; Lipotecan; RNF144A.

Abbreviations: Akt, protein kinase B; DAPI, diamidino-2-phenylindole; DDR, DNA damage repair; DNA, deoxyribonucleic acid; DNA-PK, DNA-dependent protein kinase; DNA-PKcs, DNA-dependent protein kinase, catalytic subunit; DSB, double-strand break; HCC, hepatocellular carcinoma; IHC, immunohistochemical; NHEJ, nonhomologous end-joining; NK, natural killer; pAkt, phospho-Akt; RNF, ring finger protein family; RT, radiotherapy, radiation therapy; SBRT, stereotactic body radiotherapy; TOP1, topoisomerase I.

*Correspondence to: Jason Chia-Hsien Cheng, Division of Radiation Oncology, Department of Oncology, National Taiwan University Hospital, No. 7, Chung-Shan South Rd., Taipei. ORCID: <https://orcid.org/0000-0002-2007-0220>. Tel: +886-2-2356-2842, Fax: +886-2-2331-2172, E-mail: jasoncheng@ntu.edu.tw

derivatives.

TOP1-targeted drugs have been recently shown to be the excellent radiation sensitizers.⁹ The role of camptothecin derivative-based radiosensitization is limited due to the toxicities which includes esophagitis, pneumonitis, diarrhea, nausea, and vomiting. Among TOP1i, Lipotecan is a novel camptothecin analog, synthesized with the unique lactone ring changes from camptothecin. In an *in vitro* study, Lipotecan increased radiation-induced DNA damage and inhibited DNA DSB repair in lung cancer cells.¹⁰ Lipotecan was also reported to be well tolerated and no cumulative toxicity for patients with solid tumors in a phase I trial.¹¹ The combination treatment of RT with TOP1i, such as Lipotecan, is worthy of further investigation for the potential radiosensitizing effect.¹² Until now, Lipotecan has not been approved for the clinical use.

TOP1 inhibition induces DNA-dependent protein kinase, catalytic subunit (DNA-PKcs) phosphorylation at serine 2056, required for the DSB repair.¹³ During cellular DNA damage response (DDR), DNA-PKcs acts as the active DNA-PK holoenzyme with the Ku80/Ku70 heterodimer. After DNA-PKcs is activated by phosphorylation of DDR signals, a set of downstream factors are recruited for nonhomologous end joining (NHEJ) repair and prevent the cell from apoptosis.¹⁴ The ring finger protein family is a complex set of proteins containing an RNF domain, which includes 40–60 amino acids.¹⁵ Many RNF family members have been reported to play critical roles in carcinogenesis and development. Among them, RNF144A is an E3 ubiquitin ligase for DNA-PKcs. RNF144A promotes DNA damage-induced cell apoptosis in a p53-dependent way and targets DNA-PKcs for ubiquitination and degradation.¹⁶

Patients with HCC were reported to have perturbations of Natural killer (NK) cell-related receptor/ligand axes which are an essential part of innate immunity against cancer.¹⁷ The DNA-targeting chemotherapeutics, including doxorubicin, paclitaxel, and methotrexate, upregulates the expression of major histocompatibility complex class I-related chain A and B (MICA/B) and augment NK cell-mediated cytotoxicity. Increased expression of MICA/B sensitizes cancer cells to NK cells.¹⁸ RT also upregulated MICA/B in glioblastoma models, with the upregulated MICA/B to potentially evoke immune surveillance evasion.¹⁹ The upregulated MICA/B functions as a “kill me” signal through the receptor on NK cells. This study aimed to clarify the underlying mechanism responsible for the TOP1i related DNA-PKcs/RNF144A signaling, and the enhanced immunogenicity of MICA/B in HCC.

Methods

Cell lines

Human HCC cell line Huh7 was obtained from the JCRB cell bank (Okayama, Japan), and the PLC5 cell line was obtained from American Type Culture Collection (ATCC, Manassas, VA, USA). The human NK cell line NK92 (ATCC CRL-2407) was purchased from BCRC, Hsinchu, Taiwan. NK92 cells were maintained in culture with 100 IU/ml recombinant IL-2. Cells were maintained in Dulbecco’s minimal essential Eagle medium supplemented with 10% fetal bovine serum and 50 U/ml penicillin/streptomycin. Cells were cultured at 37°C in a humidified atmosphere of 5% CO₂.

Reagents

Lipotecan was kindly provided by Taiwan Liposome Company, Ltd., (Taipei, Taiwan) as a lyophilized powder (40 mg/vial). Lipotecan was reconstituted in ddH₂O at the concentration of

100 µM. Sorafenib purchased from US Biological (#S5343-01) was reconstituted in dimethyl sulfoxide (DMSO) at the concentration of 5 mM. Irinotecan (Campto) was purchased from Pfizer Inc. (New York, NY, USA) as a ready-to-use clinical formulation solution in 5 ml vials containing 100 mg of the drug (20 mg/ml). SN-38 (ab141108) was purchased from Abcam (Cambridge, MA, USA), and MG132 (BML-PI102-0005) from Enzo Life Sciences (Farmingdale, NY, USA).

Irradiation of cells

HCC cells in culture flasks were irradiated with different doses, using a Cs-137 unit at a dose rate of 1.8 Gy/min. The source-skin-distance technique was set with 30 cm at the bottom of the flask. Dosimetry measurement was verified with an ionization chamber. Cells were plated on chamber slides and allowed to attach overnight and exposed to irradiation of 10 Gy either alone or combined with reagents, Lipotecan 10 nM or irinotecan 5 µM. After treatment, cells were incubated for 4 h and harvested for western blot or immunoprecipitation.

Colony formation assay

Cells (1,000/well) were seeded in six-well plates and treated with different doses of radiation (2.5–10 Gy) following 1-h pretreatment with various doses of Lipotecan, sorafenib, irinotecan, or DMSO vehicle. The concentrations of irinotecan for PLC5 cells and Huh7 cells were used differently. Cells were then cultured for an additional 7 days, after which the number of colonies in each well (clusters of over 50 cells) were counted using an inverted phase-contrast microscope at 100× magnification and photographed. All experiments performed independently in triplicate.

Western blot analysis

Total protein from cell lysates was extracted using Mammalian Protein Extraction Reagent (Pierce, Rockford, IL, USA). For each condition, 50 µg of protein was loaded for western blot staining. Membranes were incubated overnight at 4°C with the proper dilution of these primary antibodies: anti-RNF144A (33 kDa, HPA049939, Sigma-Aldrich, St. Louis, MO, USA), anti-phospho-DNA-PKcs (460 kDa, ab 124918), anti-DNA-PKcs (469 kDa, ab44815, Abcam, Cambridge, MA, USA) and anti-Akt (60 kDa, #9272, Cell Signaling Technology, Beverly, MA, USA). Anti-β-actin antibodies were used (42 kDa, A5441, 1:5,000; Sigma-Aldrich) to visualize protein gel loading. The appropriate horseradish peroxidase-conjugated secondary antibodies were used. All experiments repeated independently at least three times.

Subcellular fractionation

Cells were washed with phosphate buffered saline, resuspended in 400 µL of ice cold buffer (10 mM HEPES [pH 7.4], 10 mM KCl, 0.1 mM EDTA, 0.1 mM EGTA, and protease inhibitor; Roche, Mannheim, Germany), incubated on ice for 15 m to allow swelling. After adding of 25 µL of 10% NP-40, the suspension was vortexed vigorously for 10 seconds, centrifuged to pellet the nuclei, washed twice with ice cold buffer containing NP-40, and resuspended in 150 µL of 20 mM, pH 7.4 HEPES buffer (0.4 M NaCl, 1 mM EDTA, 1 mM EGTA, and protease inhibitor; Roche). Subcellular fractions containing 50 µg of protein were applied to SDS-PAGE gels for immunoblotting, as described above. The presence of endogenously expressed lamin B1 and the cytoskeleton protein α-tubulin in the nuclear and cytoplasmic fractions were shown by western blotting. All experiments were independently repeated at least three times.

Immunofluorescence microscopy

Cells were plated on polylysine-coated coverslips, allowed to attach overnight, and exposed to ionizing irradiation of 10 Gy either alone or combined with Lipotecan or sorafenib 10 nM and 0.5 μ M for Huh7 cells and 30 nM and 3 μ M for PLC5 cells. The cells were incubated for 4 h, washed three times with ice cold PBS, fixed in 4% formaldehyde/PBS for 30 m, permeabilized in 0.5% Triton X-100 in PBS for 1 h, blocked in 5% bovine serum albumin for 1 h at room temperature, incubated with fluorescein isothiocyanate (FITC) conjugated anti-phospho-histone γ -H2AX (Ser139); JBW301 05-636, 17kDa, 1:1,500 (Millipore, Billerica, MA, USA), anti-RNF144A (sc 393432), 1:200 (Santa Cruz Biotechnology, CA, USA), or anti-phospho-DNA-PKcs (ab18192), 1:600 (Abcam, Cambridge, UK) for 2 h at room temperature in the dark, washed with PBS, and mounted in Vectashield mounting medium containing diamidino-2-phenylindole (Vector Laboratories, Burlingame, CA, USA). In each sample, γ -H2AX foci were counted per nucleus using a fluorescence microscope (Axio Imager A1; Zeiss, Jena, Germany) at high magnification. The average number of γ -H2AX foci for 150 nuclei were calculated. The microscope was located at the Imaging Core Facility of the First Core Laboratory, College of Medicine, National Taiwan University. The average number of γ -H2AX foci per nucleus were the total of DSB per nucleus. All experiments were repeated independently at least three times. Colocalization analysis of RNF144A and anti-phospho-DNA-PKcs was quantified using the JACoP plugin in ImageJ.²⁰ Quantification was performed at least 150 cells per condition from three independent experiments.

Immunoprecipitation

Total cell lysates were prepared with RIPA buffer (CN89900; ThermoFisher Scientific, Waltham, MA, USA). Lysates (0.5 mg) were precleared with 40 μ L protein A/G-agarose beads (Santa Cruz Biotechnology, CA, USA) for 1 h. Protein A/G-agarose beads were added to the antibodies and rotated at 4°C for 1 h. Precleared proteins and bead-conjugated antibodies were mixed, rotated at 4°C overnight, pelleted, and washed five times with RIPA buffer. An equal volume of 6 \times Laemmli buffer was added, and the samples were boiled and separated by SDS-polyacrylamide gel electrophoresis (SDS-PAGE). All experiments were repeated independently at least three times.

Flow cytometry

Human HCC cells (5×10^6) were incubated with phycoerythrin-conjugated anti-MICA mAb (FAB1300P; R&D Systems, Minneapolis, USA), or allophycocyanin-conjugated anti-MICB mAb (FAB1599A; R&D Systems) according to the manufacturer's protocol. The fluorescence signals were detected with FACS Calibur (BD Biosciences, San Jose, CA) and analyzed with BD CellQuest Pro software. All experiments were repeated independently at least three times.

In vivo orthotopic tumor model

Male severe combined immunodeficiency (SCID) mice 6 weeks of age were obtained from the Animal Center of National Taiwan University. All experimental procedures were approved by National Taiwan University Institutional Animal Care and Use Committee. Huh7 cells (1×10^5) were injected directly into the left hepatic lobe. One week after tumor cell injection, 36 mice were randomized to: (1) control treatment (vehicle), (2) intravenous Lipotecan (40 mg/kg/day on days 0, 4, and 8), (3) oral sorafenib (20 mg/kg/day on days 0–9), (4) RT (5 Gy daily on days 1, 4, and 9), (5) the combination

of Lipotecan and RT, and (6) the combination of sorafenib and RT. Living Image software was used to process the bioluminescent signals and generate growth curves of liver tumors once a week from weeks 0 to 3. Mice from each group were sacrificed 3 weeks after treatment.

Radiotherapy to orthotopic liver tumor

Mice were immobilized, simulated, and irradiated with a half-beam rectangular field to the left two-thirds of the liver covering the tumor. A 6-MV photon linear accelerator and a small animal X-ray irradiator (X-RAD SmART small animal radiotherapy; Precision, Madison, CT, USA) was used to irradiate the liver tumor with three fractions of 5 Gy/day on days 1, 4, and 9.

Immunohistochemical staining

Mice from each group were sacrificed on day 21. The tumor was fixed in 10% neutral buffered formalin and processed for histopathological and immunohistochemical staining. After fixation, tumor tissues were embedded in paraffin blocks and sectioned (5 μ m). Tumor cells were detected in representative stained sections. The expression of phospho-DNA-PKcs (#74965), phospho-Akt (#4060), cleavage caspase 3 (#9964; Cell Signaling Technology, Beverly, MA, USA), and MICA/B (ab203679; Abcam, Cambridge, UK) were evaluated after immunohistochemical staining with specific antibodies. Pictures were recorded using a Zeiss AxioImager microscope. Images of immunohistochemical staining with MICA/B were analyzed in an unsupervised and blinded fashion using TMAPKER, a software toolkit for histopathologic staining estimation.²¹ Immunoreactivity was analyzed by three investigators.

Statistical analysis

All experiments were repeated at least three times. Statistical analysis was carried out using an unpaired two-tailed Student's *t*-test or the Mann-Whitney rank-sum test. *P*-values <0.05 were considered significant.

Results

Superior radiosensitizing effect of TOP1i to RT but different efficacy on clonogenicity in two HCC cell lines

To investigate the potential role of TOP1i in HCC radiosensitization, we first compared the synergistic effect of a novel TOP1i Lipotecan with RT. Radiotherapy combined with Lipotecan had a significant synergistic effect on clonogenicity in two human HCC cell lines, Huh7 and PLC5. In clonogenic survival assays, the combination of radiation (2.5–10 Gy) and Lipotecan treatment (2.5–12.5 nM in Huh7 cells, 7.5–37.5 nM in PLC5 cells) induced a noticeable dose-dependent reduction of cell viability (Fig. 1A), and was more effective in Huh7 than PLC5 cells. To confirm the similar radiosensitizing effect by another TOP1i, the combination of radiation and irinotecan (0.1–0.5 μ M in Huh7 cells, 0.5–2.5 μ M in PLC5 cells), a common TOP1i in clinical use, also induced differential dose-dependent reduction of cell viability (Supplementary Fig. 1) in both cell lines.

Lipotecan induces radiation-induced DNA damage

Phosphorylated H2AX (γ -H2AX) generated at the foci of radiation-induced DSB is one of the gold standards for estimating DSB. To analyze differences of DNA damage by Lipotecan, γ -H2AX foci per cell was counted in Huh7 and PLC5 cells treated with radiation (10 Gy) alone, and combined radia-

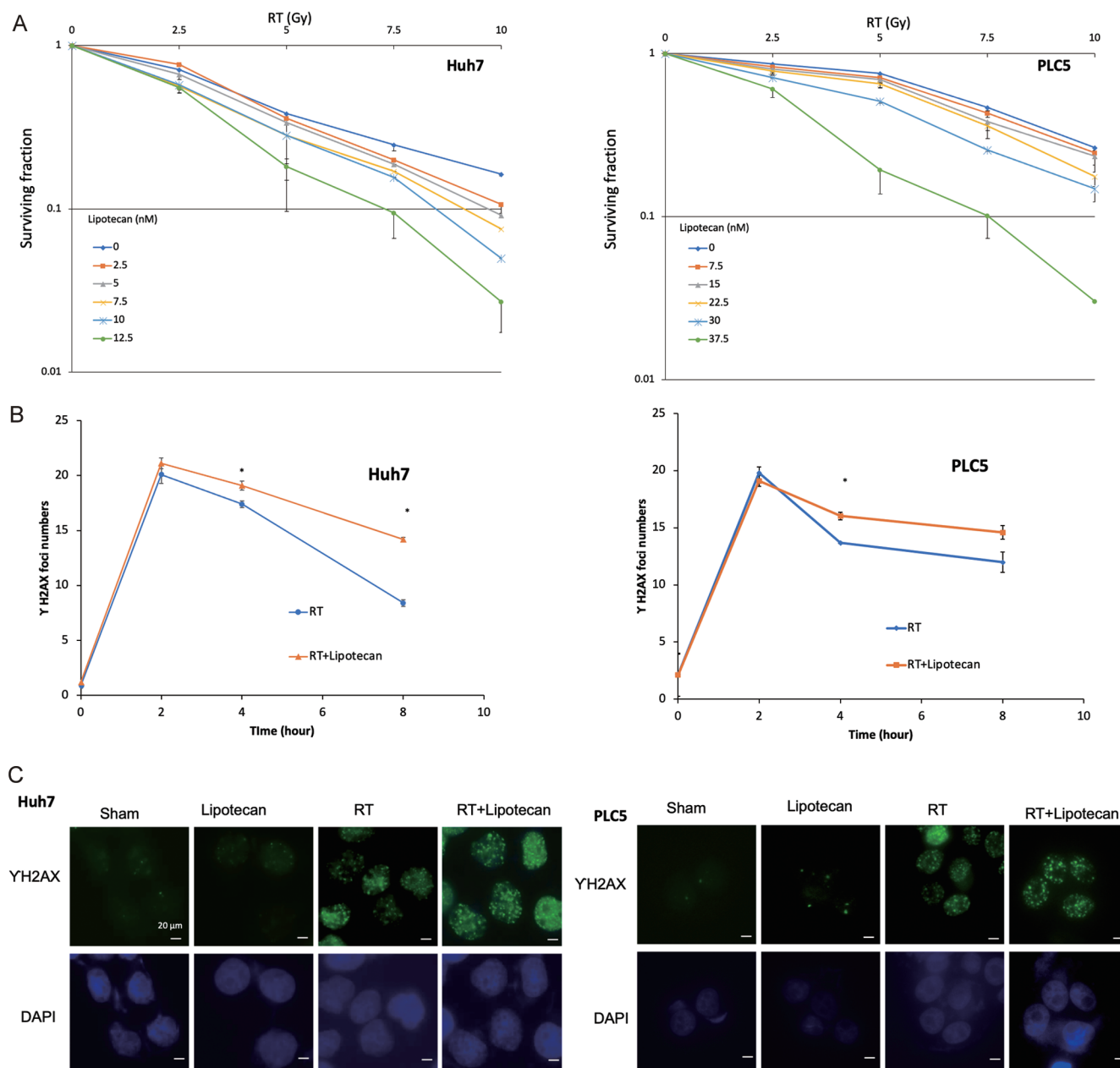


Fig. 1. Radiosensitizing effect of topoisomerase 1 inhibitor (TOP1i, Lipotecan) on hepatocellular carcinoma (HCC) cells. (A) Lipotecan enhances the radiosensitization of HCC cell lines, Huh7 better than PLC5 in clonogenic survival assays. Cells were seeded in six-well plates and treated with different doses of radiation (2.5–10 Gy) following 1-h pretreatment with various doses of Lipotecan, or dimethyl sulfoxide vehicle. Cells were then cultured for an additional 7 days. The surviving fraction was determined as described in Material and Methods. All experiments were performed independently in triplicate. Quantitative results of clonogenic assays after combination treatment with Lipotecan and irradiation (RT). Data in the graph are means \pm SD. At each dose level, the colony count is expressed as a fraction of the number in the corresponding control group. (B) The average number of γ -H2AX foci after RT-induced DNA damage with/without Lipotecan in Huh7 and PLC5 cells, $*p < 0.05$. (C) Representative immunofluorescence images of γ -H2AX formed in the nuclei of Huh7 and PLC5 cells treated by sham, Lipotecan, RT, and combined RT/Lipotecan are shown. Each cell line was exposed to ionizing irradiation of 10 Gy either alone or combined with Lipotecan. The Lipotecan concentrations were 10 nM for Huh7 cells, and 30 nM for PLC5 cells. The cells were then incubated for 4 h before harvest. Data are from a representative experiment of at least triplicate.

tion and Lipotecan. At 4 h, the combined Lipotecan increased the number of γ -H2AX foci/cell by 1.1-fold compared with radiation alone (19.1 ± 0.4 vs. 17.4 ± 0.3 , $p < 0.05$) in Huh7 cells. The difference remained significant at 8 h by 1.7-fold (14.2 ± 0.2 vs. 8.4 ± 0.3 , $p < 0.05$; Fig. 1B). In PLC5 cells, Lipotecan increased the number of γ -H2AX foci/cell by 1.17-fold compared with radiation alone (18.0 ± 0.3 vs. 13.7 ± 0.1 ,

$p < 0.05$) at 4 h.

TOP1 inhibitor better synergizes the antitumor effect of RT

To confirm the *in vivo* antitumor effect of RT combined with TOP1i (Lipotecan), we used a SCID mouse model bearing an orthotopic liver tumor. All mice were implanted with 1×10^5

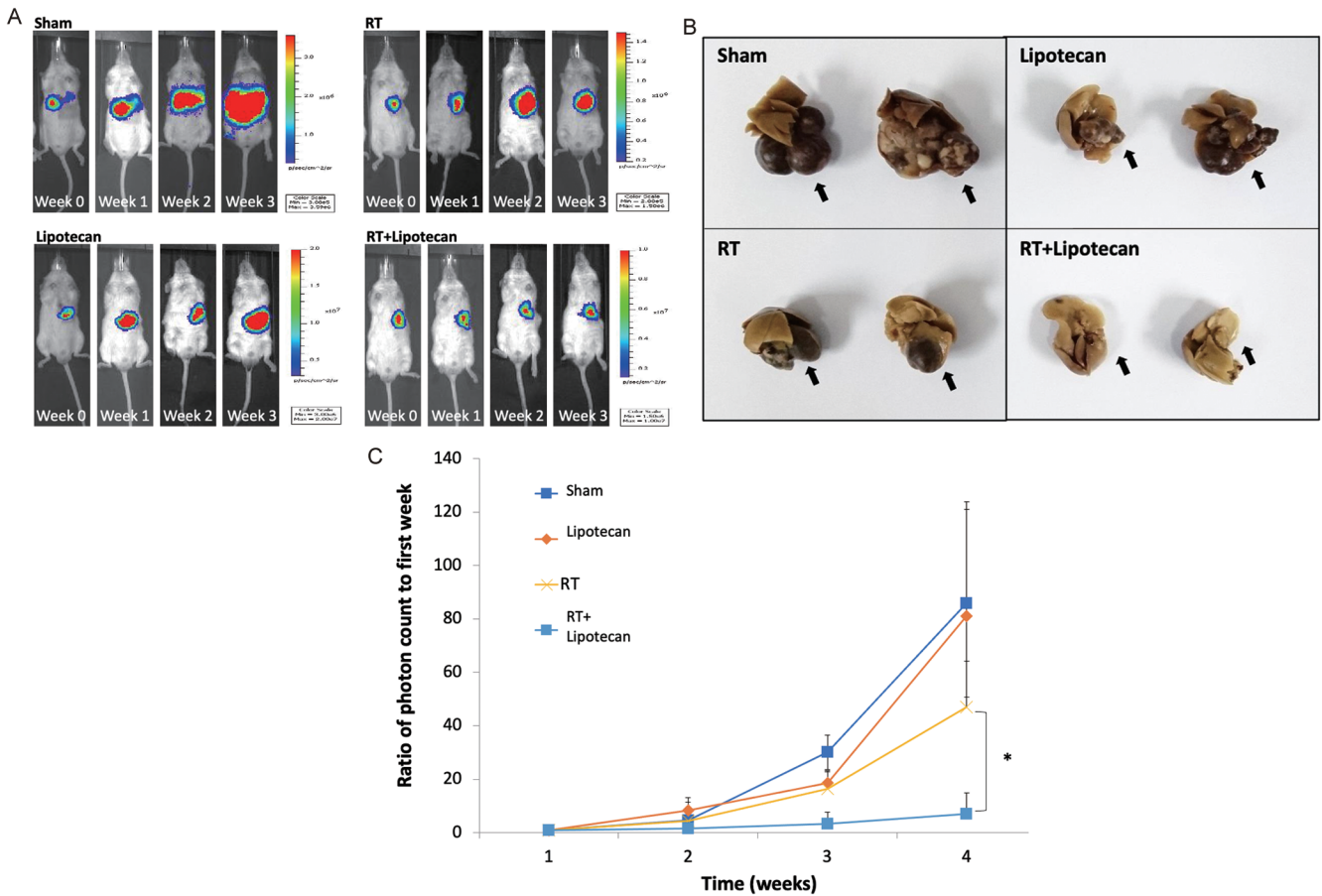


Fig. 2. Radiotherapy (RT) combined with topoisomerase 1 inhibitor (TOP1, Lipotecan) inhibited orthotopic liver xenograft tumor models in severe combined immunodeficient mouse. Huh7 cells (1×10^5) were injected directly into the left hepatic lobe. One week after the tumor cell injections, mice were randomized to: (1) sham treatment (vehicle), (2) intravenous Lipotecan, (3) RT, and (4) the combination of Lipotecan and RT. Tumor growth was tracked and measured by xenogen bioluminescence imaging. (A) Representative xenogen imaging results of one representative bioluminescence image in each group from week 0 to 3 are shown. Color bars represent tumor cell intensity from low (blue) to high (red). (B) Photographs livers dissected on day 21 from two representative mice in each group. Black arrows indicate the liver tumor. (C) The combination of RT and Lipotecan significantly reduced tumor growth by 7-fold compared with RT alone ($p < 0.05$) at the end of week 3. Data are mean \pm SD ($n=6$ for each group; $*p < 0.05$, $**p < 0.01$, compared with RT and Lipotecan, *t*-test). All experiments were repeated independently at least three times.

Huh7Fluc cells by injection into the parenchyma of the left hepatic lobe. After the activity of luciferase, tumor reached the threshold level, 24 mice were randomly divided into four groups: (1) control treatment (vehicle), (2) intravenous Lipotecan (40 mg/kg/day on days 0, 4, and 8), (3) RT (5 Gy daily on days 1, 4, and 9), and (4) the combination of Lipotecan and RT. *In vivo* bioluminescent imaging was used weekly to evaluate the antitumor effect. Figure 2A shows representative bioluminescence images of the tumor response in each group between weeks 0 and 3. The imaging data of livers dissected from two representative mice in each group in Figure 2B illustrate the consistent between-group differences. A comparable tumor growth pattern was seen in each group. The combination of RT and Lipotecan significantly reduced tumor growth by 7-fold compared with RT alone ($p < 0.05$) at the end of week 3 (Fig. 2C). The data confirmed that the combination treatment of RT and Lipotecan improved the control of orthotopic liver tumors more effectively than the other treatment groups.

Using immunohistochemical (IHC) staining, a reduction of radiation-activated pDNA-PKcs and pAkt was found in orthotopic HCC tumors. The combination treatment of RT and

Lipotecan significantly suppressed the expression of pDNA-PKcs and pAkt compared with RT alone (Supplementary Fig. 2A, B). In addition, IHC staining of caspase 3 showed that combined RT and Lipotecan increased apoptosis in the orthotopic tumors (Supplementary Fig. 2C). IHC staining of pDNA-PKcs, pAkt, and caspase 3 did not differ following the RT alone or RT plus sorafenib. The results indicate that Lipotecan radiosensitized HCC xenografts *in vivo* via impairing DNA-PKcs and Akt-dependent DNA DSB repair and inducing caspase 3-related apoptosis. The *in vivo* Huh7 xenografts had increased γ -H2AX and RNF144A expression after radiation combined with TOP1i as in the *in vitro* results (Supplementary Fig. 2D, E).

TOP1i inhibits radiation-activated DNA-PKcs and Akt signaling of Huh7 but not PLC5 cells

To investigate the molecular mechanism of TOP1i on radiation-induced DNA-dependent protein kinase, catalytic subunit (DNA-PKcs), and Akt phosphorylation, Huh7 and PLC5 cells were treated with Lipotecan at the indicated concentrations. Phosphorylated DNA-PKcs (pDNA-PKcs) and phosphorylated Akt (pAkt) were then assayed by western blotting.

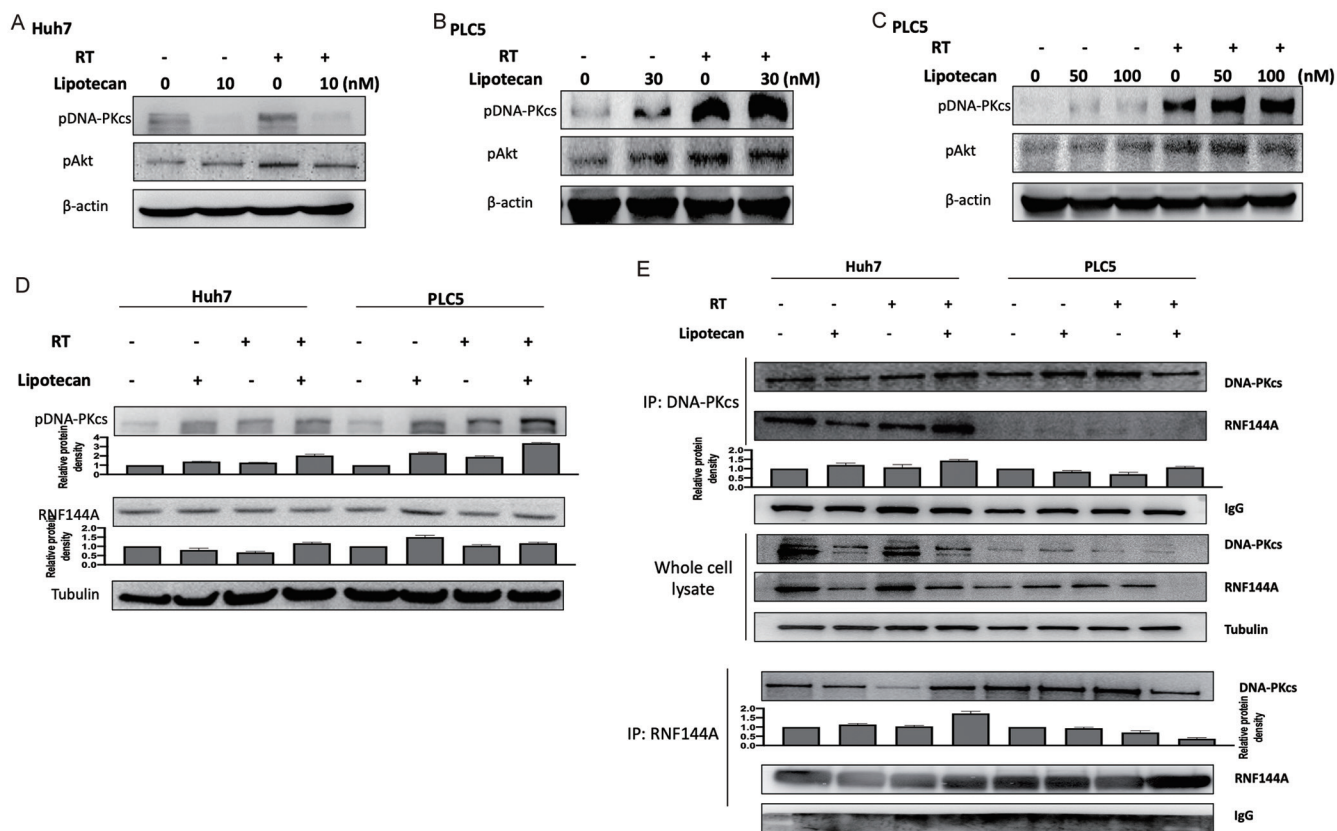


Fig. 3. Topoisomerase 1 inhibitor (TOP1i) inhibits radiation (RT)-activated DNA-dependent protein kinase, catalytic subunit (DNA-PKcs) signaling in Huh7 but not PLC5 cells. Western blotting (WB) showed that the levels of phosphorylated DNA-PKcs (pDNA-PKcs) increased after RT and were inhibited by Lipotecan in (A) Huh7 but not (B) PLC5 cells. (C) The inhibitory effect of radiation-induced phosphorylated DNA-PKcs (pDNA-PKcs) was not observed with higher doses of Lipotecan (50 nM and 100 nM) in irradiated PLC5 cells. (D) Phosphorylated DNA-PKcs increased after RT and was inhibited by Lipotecan in Huh7 cells but not in PLC5 cells. WB shows that the levels of RNF144A increased after RT and were inhibited by Lipotecan, in Huh7 cells but not in PLC5 cells. (E) After Lipotecan with/without RT, RNF144A was detected by WB in immunoprecipitates (IPs) with antibody to DNA-PKcs in Huh7 and PLC5 cells (upper three panels). DNA-PKcs were detected by WB in IP with antibody to RNF144A after Lipotecan with/without RT in Huh7 and PLC5 cells (lower three panels). Cells were exposed to ionizing irradiation of 10 Gy either alone or combined with Lipotecan 10 nM. After treatment, cells were incubated for 4 h and harvested for WB or IP. Data are means \pm SD from a representative experiment of at least triplicate.

Interestingly, the combination of radiation and Lipotecan inhibited radiation-activated pDNA-PKcs and pAkt expression in Huh7 (Fig. 3A) but not in PLC5 cells (Fig. 3B). To confirm the difference, higher doses of Lipotecan (50 nM and 100 nM) were used in irradiated PLC5 cells. Despite the reduction of radiation-activated pAkt, the inhibitory effect of Lipotecan on radiation-activated pDNA-PKcs was still not shown in PLC5 cells (Fig. 3C).

RNF144A mitigates the prosurvival function of radiation-induced DNA-PKcs phosphorylation after TOP1i

DNA-PKcs is an integral part of nonhomologous DNA end joining (NHEJ) promoting cell survival after radiation injury.²² RNF144A is an E3 ubiquitin ligase for DNA-PKcs that increases DNA damage-induced cell apoptosis.²³ To understand the possible mechanism that controls the expression of DNA-PKcs, the changes of RNF144A after RT and TOP1i (Lipotecan and irinotecan) were analyzed in the two HCC cell lines. With the increased expression of phosphorylated DNA-PKcs after radiation, Lipotecan (Fig. 3D) and irinotecan (Supplementary Fig. 1C) inhibited RT-activated DNA-PKcs signaling in Huh7 but not in PLC5 cells. The expression of RNF144A was activated after radiation combined with irinotecan in Huh7 cells but not in PLC5 cells (Fig. 3D and Supplementary Fig. 1C).

The active metabolite of irinotecan, SN38, also inhibited the expression of radiation-induced DNA-PKcs and activated the expression of RNF144A in Huh7 but not in PLC5 cells (Supplementary Fig. 4). So it was assumed that the RNF144A is counteracting the effect of DNA-PKcs.

Interaction of DNA-PKcs and RNF144A after TOP1i with/without irradiation

Co-immunoprecipitation was performed to check the interaction of DNA-PKcs and RNF144A-related ubiquitination after TOP1i and/or radiation. HCC cells were treated with Lipotecan/irinotecan and/or radiation and whole-cell extracts were prepared for the immunoprecipitation assay. The extracts were immunoprecipitated with antibody to DNA-PKcs had RNF144A and vice versa. RNF144A DNA-PKcs increased after combined Lipotecan and radiation in Huh7 cells but decreased in PLC5 cells (Fig. 4C). RNF144A DNA-PKcs also increased after combined Lipotecan and radiation in Huh7 cells but decreased in PLC5 cells (Fig. 3E). A similar effect was seen after combined irinotecan and radiation in Huh7 and PLC5 cells (Supplementary Fig. 1D, E). The data show that RNF144A targeted DNA-PKcs in Huh7 cells for ubiquitination and degradation during DNA damage after TOP1i and radiation. That shows for the first time that RNF144A-related ubiquitination

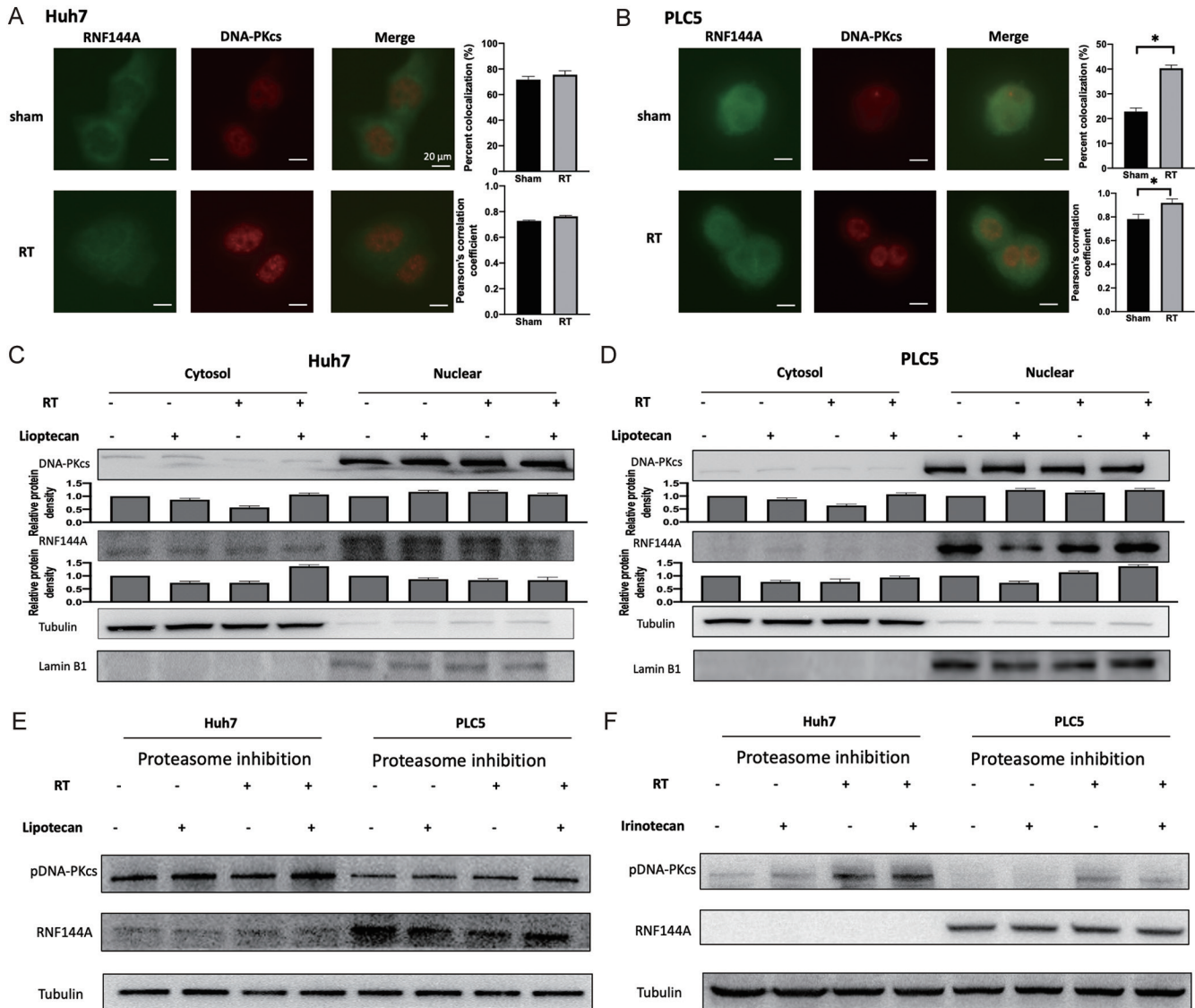


Fig. 4. Nuclear translocation of RNF144A. In (A) Huh7 and (B) PLC5 cells after radiation (RT) by co-immunofluorescence staining with the indicated antibodies. Yellow fluorescence formed by the overlap of red and green fluorescence indicated the colocalization of DNA-PKcs and RNF144A in the cytoplasm. After treatment with Lipotecan 10 nM and/or RT 10 Gy, cells were processed at 4 h to isolate and measure the cytosolic and nuclear protein fractions. Percent colocalization and Pearson's correlation coefficient are shown in the bar graph of means \pm SD, unpaired two-tailed Student's *t*-test. **p*<0.05. Nuclear and cytosolic proteins were used for western blotting (WB) assays with antibodies against DNA-PKcs and RNF144A in (C) Huh7 and (D) PLC5 cells. The proteasome inhibitor, MG132 20 μ M 2 h before harvest, reversed the differential effect of the phosphorylated DNA-PKcs catalytic subunit (pDNA-PKcs) and RNA144A in (E) Huh7 and (F) PLC5. Data are means \pm SD from a representative experiment of at least triplicate.

may be responsible for the differential response in Huh7 and PLC5 cells to combined treatment.

Differential effect on nuclear translocation of RNF144A in Huh7 and PLC5 cells after radiation and TOP1 inhibition

The location of the DNA-PK complex has been reported to be a critical factor involving DNA damage/repair machinery after RT.²⁴ Hence, change in the localization of the RNF144A/DNA-PKcs complex after DNA damage was investigated. First, the subcellular localization of RNF144A was characterized by using indirect immunofluorescence. After RT, nuclear translocation of RNF144A was seen in PLC5 cells (Fig. 4B) but not in Huh7 cells (Fig. 4A) by staining of RNF144A and

DNA-PKcs. Yellow fluorescence in the cytoplasm formed by the overlap of red and green fluorescence indicated that the colocalization of DNA-PKcs and RNF144A, showed ubiquitination of DNA-PKcs by RNF144A acting in the cytoplasm. Next, the nuclear and cytosolic proteins were separated for western blotting assay with antibodies against DNA-PKcs and RNF144A proteins. Similarly, intranuclear accumulation of RNF144A was seen after combining RT with Lipotecan in PLC5 cells (Fig. 4D), compared with the increased expression of RNF144A in the cytoplasm of Huh7 cells (Fig. 4C). Also, increased expression of DNA-PKcs was shown in the cytoplasm of PLC5 cells (Fig. 4D). A similar effect was also shown with treatment of irinotecan and/or radiation in Huh7 (Supplementary Fig. 3A) and PLC5 cells (Supplementary Fig. 3B).

Reverse effects with proteasome inhibition on phosphorylated DNA-PKcs and RNF144A after combining TOP1i and radiation

In mammalian cells, proteasomes control the degradation of ubiquitin-conjugated proteins.²⁵ We investigated whether inhibiting the ubiquitin/proteasome system with MG132, a potent and reversible proteasome inhibitor, increased the expression of pDNA-PKcs in Huh7 cells after combined TOP1i and radiation. With proteasome inhibition, the differential effects of combined Lipotecan and radiation in Huh7 and PLC5 cells (Fig. 4E) and with combined irinotecan and radiation on pDNA-PKcs and RNF144A were reversed (Fig. 4F).

TOP1i radiosensitizes HCC cells to NK cell-mediated killing and upregulates radiation-induced MICA/B expression

NK cells cocultured with HCC cells increased the radiosensitizing effect by TOP1i, Lipotecan (Fig. 5A). The effects of RT on MICA/B expression in HCC cells were shown by the increase of major histocompatibility complex class I chain-related protein A MICA expression by 1.18 fold and 1.36 fold with RT and combined RT/Lipotecan in Huh7 cells, and 1.14 fold and 1.47 fold in PLC5 cells. Increases of MICB expression were 1.30-fold with RT and 1.36-fold with combined RT/Lipotecan in Huh7 cells, and 1.07-fold and 1.26-fold in PLC5 cells (Fig. 5B–D). In orthotopic HCC tumors, the expression of MICA/B also increased significantly with RT and/or Lipotecan on IHC staining ($p < 0.01$; Fig. 6A, B). Taken together, the results indicate that DNA-PKcs increased in response to radiation-induced DNA damage. TOP1i mediated the ubiquitination and degradation of cytosolic DNA-PKcs regulated by RNF144A, and accounts for the differential radiosensitizing effect in Huh7 and PLC5 cells. In Huh7 cells, combining radiation with TOP1i increased DNA-PKcs ubiquitination by RNF144A, suppressed subsequent DNA repair, and resulted in a better radiosensitizing effect. In PLC5 cells, the combined treatment induced RNF144A nuclear translocation with fewer DNA-PKcs ubiquitination/degradation. Intranuclear accumulation of RNF144A and increased cytosolic DNA-PKcs may be involved in DNA repair for less effective cytotoxicity. The combination of RT and TOP1i enhanced the expression of MICA/B ligands to sensitize the NK cell-mediated killing effectiveness of HCC cells (Fig. 6C).

Discussion

With the advancement of technology, RT has become one of the treatment options for localized HCC not suitable for or refractory to conventional treatments.³ Despite the intra-arterial approach by yttrium-90 and increased dose intensity by stereotactic body RT (SBRT), radiotherapeutic effects remain unsatisfactory.²⁶ The inhibition of radiation-activated signaling pathways to overcome the sublethal effect may be a strategy to enhance the therapeutic effect of RT on hepatic tumors.⁴ Sorafenib, a multikinase inhibitor that blocks c-RAF vascular endothelial growth factor and platelet-derived growth factor-a kinases, is the first systemic treatment with a proven survival benefit for advanced HCC. Several pre-clinical studies investigated the radiosensitizing effect of sorafenib *in vitro* and *in vivo*.^{6,27} However, combined treatment with RT and sorafenib in unresectable HCC showed toxicities in clinical use.^{7,28} In this study, TOP1i was shown as a more potent radiosensitizer than sorafenib for HCC. The mechanism of radiosensitization by TOP1i was by ubiquitination of radiation-induced DNA-PKcs by RNF144A to interfere with DNA-PKcs-related DNA repair, resulting in an enhanced

lethal effect in HCC. This study also demonstrated a differential radiosensitizing effect in two HCC cell lines with different amounts of ubiquitination of DNA-PKcs and nuclear translocation of RNF144A.

Effects of TOP1i

DNA is the critical target of radiation, and DSB in DNA is the primary lethal lesion after RT. Nuclear DNA TOP1 is an essential enzyme involved in DNA DSB repair.⁸ Irinotecan stabilizes cleavable TOP1-DNA complexes, which results in DNA damage and apoptosis of cancer cells. *In vitro* studies showed SN38, the active metabolite of irinotecan, had promising anticancer effectiveness in HCC.²⁹ Irinotecan is the first-line chemotherapy in patients with various solid tumors, including colorectal³⁰ and pancreatic cancer.³¹ However, the response to irinotecan in HCC patients was not satisfactory.⁹ Clinical studies of TOP1i have not shown a significant benefit in patients with HCC because of dose-dependent toxicity.³² Clinical trials of other agents and irinotecan used a lower dose to improve safety and efficacy.³³ Recent findings support the use of the TOP1i as a promising combination treatment for HCC.³⁴

DNA-PKcs and radiosensitization

Accumulating evidence indicates the critical role of DNA-PKcs in HCC development and progression.³⁵ DNA-PKcs have an important role in the NHEJ DNA repair pathway and provides pro-survival signaling during DNA damage. Activation of DNA-PKcs requires the phosphorylation of specific amino acid residues in its catalytic subunit, in which T2609 and S2056 have been identified to be essential for NHEJ repair of DNA DSBs.³⁶ Likewise, deletion of these phosphorylation sites results in enhanced cellular sensitivity to irradiation.³⁷ Lipotecan inhibited autophosphorylation of DNA-PKcs S2056 in Huh7 cells, which became more sensitive to radiation. In NHEJ, broken DNA ends are bound with high affinity by the Ku70/Ku80 heterodimer followed by recruitment and activation of the DNA-PKcs.³⁸ This study showed that TOP1i suppressed radiation-induced DNA-PKcs and had a better anticancer and radiosensitizing effect than sorafenib, the most common targeted drug in advanced HCC (Supplementary Figs. 5 and 6).

RNF144A and DNA repair

RNF144A, the E3 ubiquitin ligase for DNA-PKcs, is mainly localized in the cytoplasmic vesicles and plasma membrane and interacts with cytoplasmic DNA-PKcs.³⁹ It mediates the ubiquitination of DNA-PKcs and promotes apoptosis upon DNA damage. Depletion of RNF144A leads to an increased level of DNA-PKcs and resistance to DNA damaging agents, which is reversed by DNA-PKcs inhibitors.²³ RNF144A is involved in apoptosis by downregulation of DNA-PKcs when cells suffer from persistent or severe DNA damage insults.⁴⁰ In this study, TOP1 inhibitors increased the ubiquitination of DNA-PKcs in Huh7 cells and conjugated with RNF144A. In contrast, increased translocation of RNF144A to the nucleus was seen in PLC5 cells. Such differences between Huh7 and PLC5 cells might be responsible for their differential response to a combined treatment of RT and TOP1 inhibitors.

The ubiquitin-proteasome system

RNF144A involves the ubiquitination of DNA-PKcs and its degradation in proteasomes.²³ The ubiquitin-proteasome system (UPS) plays a key role in the processes of the cell cycle, apoptosis, receptor signaling, endocytosis, and many others.⁴¹ Several molecular analyses of HCC have highlighted many genetic and epigenetic changes influenced by the UPS.

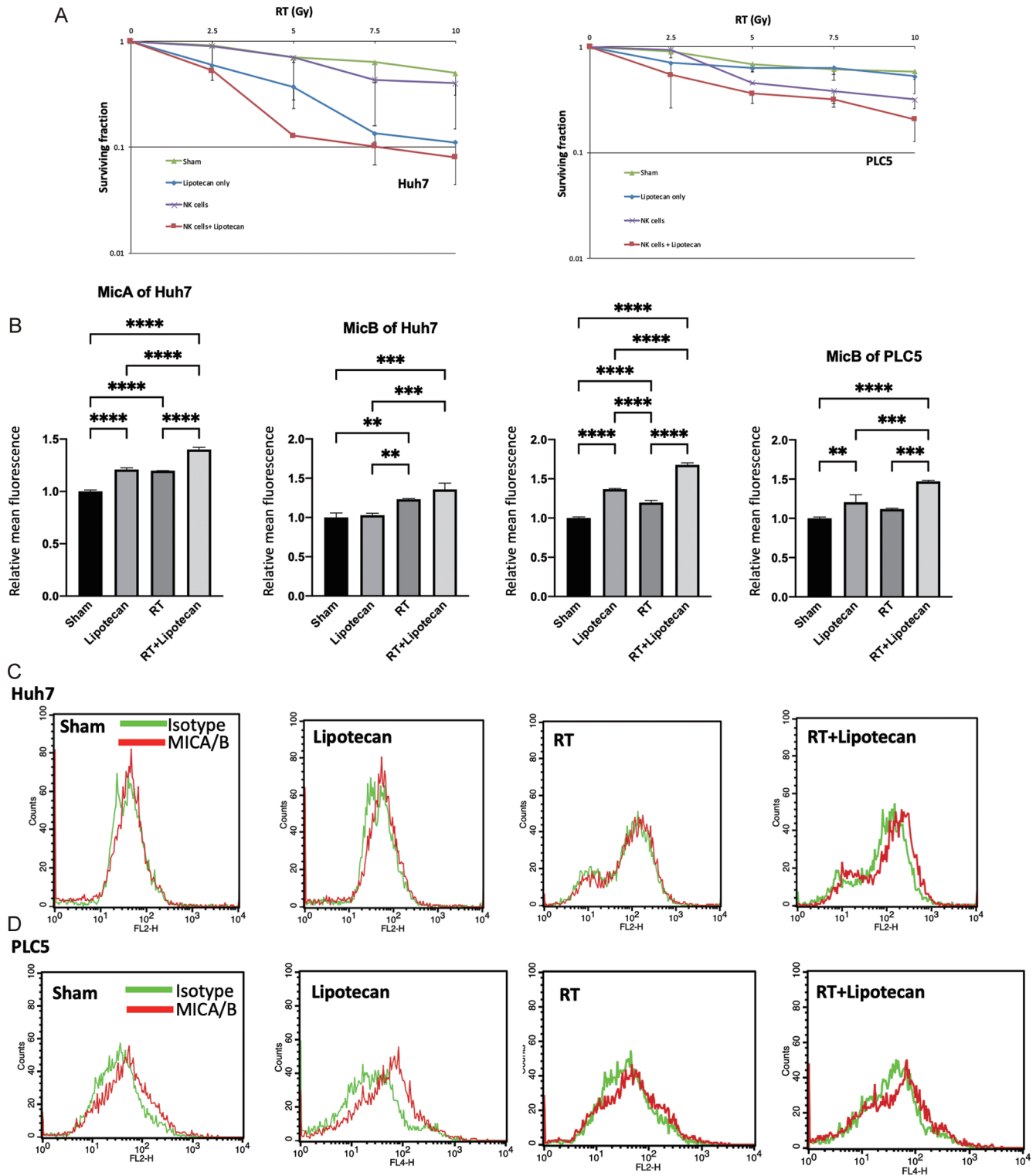
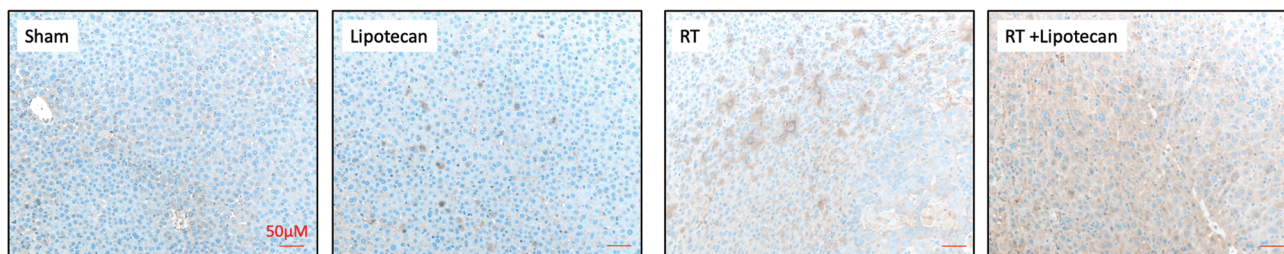
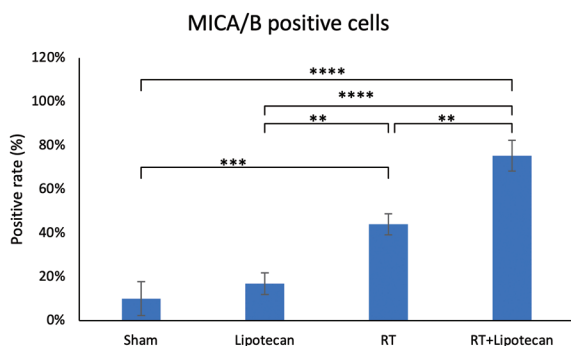


Fig. 5. TOP1-inhibition radiosensitized HCC cells to NK cell-mediated killing and upregulates radiation-induced MICA/B expression. (A) HCC cells pretreated with Lipotecan and/or radiation were cocultured with NK92 cells. Cells were seeded and treated with different doses of radiation (2.5–10 Gy) following 1-h pretreatment with Lipotecan, or DMSO vehicle. Cells were then cocultured with NK92 cells for an additional 7 days. The surviving fraction was determined as described in Materials and Methods. All experiments were performed independently in triplicate. (B) Quantitative results of HCC cells treated with Lipotecan and/or radiation for 24 h were immunolabeled with anti-MICA or anti-MICB antibodies and fluorescent signals were detected by flow cytometry analysis (C) Huh 7 and (D) PLC 5 cells with the isotype controls shown as green histograms. ** $p < 0.01$, *** $p < 0.001$, and **** $p < 0.0001$. Data are means \pm SD from a representative experiment of at least triplicate.

A IHC: MICA/B



B



C

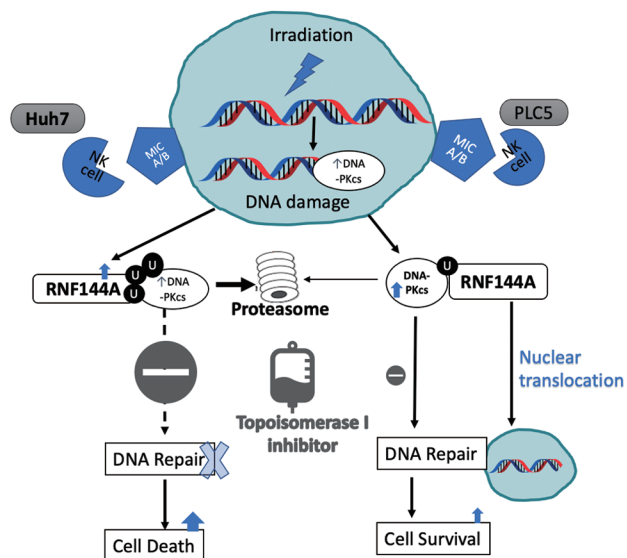


Fig. 6. Radiation-induced MICA/B expression *in vivo* and schematic diagram of NK cell-mediated differential cytotoxic radiosensitizing effects of topoisomerase 1 (TOP1) inhibition. (A) Immunohistochemical (IHC) staining of MICA/B in cross-sections of orthotopic liver tumors in (1) sham treatment (vehicle), (2) intravenous Lipotecan, (3) RT, and (4) the combination of Lipotecan and RT. (B) Percentage of MICA/B expression from the representative cross-sections. (C) Diagram of NK cell-mediated cytotoxic and differential radiosensitizing effects after RT combined with topoisomerase 1 (TOP1) inhibition of RNF144A-mediated DNA-PKcs ubiquitination and DNA repair pathways in Huh7 and PLC5 cells. ** $p < 0.01$, *** $p < 0.001$, and **** $p < 0.0001$. Data are means \pm SD from a representative experiment of at least triplicate.

The UPS has been a novel target for drug development. Bortezomib, a proteasome inhibitor, was tested combined with doxorubicin for patients with advanced HCC in a phase II trial, but the primary endpoint of objective response was not met.⁴² Bortezomib sensitized HCC cells to RT by the inhibition of protein phosphatase 2A (CIP2A).⁴³ CIP2A regulates the activity of serine/threonine protein phosphatases that control Akt and ERK. Although DNA-PK is a nucleolus protein, the catalytic subunit, DNA-PKcs is abundant in the cytoplasm.⁴⁴ RNF144A was reported to induce the ubiquitination and degradation of cytoplasmic DNA-PKcs during DDR.¹⁶ To prevent the therapeutic effect of the proteasome inhibitor, a low dose of MG132 was used, to test the molecular mechanism on RT. The findings were consistent with previous studies showing that the low-dose proteasome inhibitor increased the accumulation of DNA-PKcs in Huh7 cells.

Immune recognition receptors of MICA/B

Combining targeted therapy with immunotherapy results in a potentially additive benefit in several types of cancer, including HCC.⁴⁵ Stimulation of the receptors on tumor cells improves tumor control through the immune recognition functions of NK and T cells.⁴⁶ Available evidence suggests that RT improves the antitumor effect of immunotherapy.⁴⁷ The malignant potential of HCC including proliferation, invasion, and

metastasis, are closely related to cellular immune function. NK cells are the major cytolytic effectors in innate immunity.⁴⁸ RT was reported to enhance the NK-cell-induced anti-tumor effect in leukemia.⁴⁹ In solid tumors, RT was shown to increase immune-priming for a better response to immunotherapy.⁵⁰ MICA/B is a vital signal to induce anti-tumor immunity during HCC carcinogenesis.⁵¹ Our findings indicated the increased expression of MICA/B expression in HCC cells treated with RT and Lipotecan and in orthotopic HCC tumors.

Limitations

The study has some limitations. First, it did not provide evidence regarding the direct knockdown of the target genes, RNF144A. Instead, using TOP1i is commonly seen in other studies,²³ and we have a complete data set for the effectiveness of TOP1i, Lipotecan, and irinotecan. Second, this study did not expand the application of RNF144A as a predictive marker in patients undergoing HCC treatment. The ways to develop RNF144A as a predictive or prognostic marker for radiosensitization are still under investigation. Third, the comprehensive interaction with DNA damage/repair after nuclear translocation of RNF144A in PLC5 cells is not clear. Studies are ongoing to discover the determining function of RNF144A in the nucleus. Fourth, the dose-response mechanism of NK cell-mediated cytotoxicity by combined RT/Lipotecan remains

to be determined. Low-dose RT had a tendency to increase the function of NK cells and high-dose RT decreased the function. During RT for HCC, high-dose RT always focused on the tumor and low-dose RT spread to nearby normal liver tissue. A low dose to the normal liver might boost the cytotoxicity of NK cells. Fifth, the SCID mouse model used in this study had no T and B cells, had abundant innate immune system components like NK cells, macrophages, granulocytes, and complement proteins. Karube *et al.*,⁵² reported that phosphorylated Akt levels in NK cell lines were significantly lower than in other cell lines. The majority of the pDNA-PKcs and pAkt expressions in our study were found in the tumor (Supplementary Fig. 2). Tumor cells, rather than infiltrating immune cells, were thought to be the source of pDNA-PKcs and pAkt production. However, we cannot confirm that in this study.

Conclusion

DNA-PKcs has a prosurvival function in the repair pathway after RT-induced DNA damage. In this study, Lipotecan a novel TOP1 inhibitors, was a radiosensitizing agent that mediated the ubiquitination and degradation of DNA-PKcs by RNF144A, which was responsible for the differential radiosensitizing effects in two HCC cell lines. TOP1 inhibitors have the potential to act synergistically with RT for immune-priming in HCC immunotherapy.

Acknowledgments

We thank the staff of the Eight Core Labs, Department of Medical Research, and National Taiwan University Hospital, for their technical support during the study. We thank the staff of the imaging core at the First Core Labs, National Taiwan University College of Medicine, for technical help. We also thank Dr Pei-Jer Chen for critical reading of the manuscript.

Funding

This work was supported by National Taiwan University Hospital (NTUH 106-M3649, 107-M4030, 108-M4213, 109-M4767 and 110-M5149) and the Ministry of Science and Technology of Taiwan (MOST 106-2314-B-002-063-, 107-2314-B-002-097- and 108-2314-B-002-046-).

Conflict of interest

WNY is a full-time employee of Taiwan Liposome Company. JCHC has been an editorial board member of *Journal of Clinical and Translational Hepatology* since 2021. The other authors have no conflict of interests related to this publication.

Author contributions

Designed, performed, and analyzed the experiments, obtained funding for the project, compiled the figures and wrote the manuscript (CLT, JCHC), analyzed the experiments, compiled the data, and performed statistical analysis/designed the figures (PSY, FMH), analyzed the data and critically reviewed the manuscript (ALC, WNY), read and approved the final version (all authors).

Ethical statement

The protocols for procedures in mice were approved by the National Taiwan University Institutional Animal Care and Use Committee and conformed to the Guide for the Care and Use

of Laboratory Animals published by the National Institutes of Health.

Data sharing statement

The raw data supporting the conclusions of this article are available from the corresponding author upon request.

References

- Bray F, Ferlay J, Soerjomataram I, Siegel RL, Torre LA, Jemal A. Global cancer statistics 2018: GLOBOCAN estimates of incidence and mortality worldwide for 36 cancers in 185 countries. *CA Cancer J Clin* 2018;68(6):394–424. doi:10.3322/caac.21492, PMID:30207593.
- Deng ZJ, Li L, Teng YX, Zhang YQ, Zhang YX, Liu HT, *et al.* Treatments of Hepatocellular Carcinoma with Portal Vein Tumor Thrombus: Current Status and Controversy. *J Clin Transl Hepatol* 2022;10(1):147–158. doi:10.14218/JCTH.2021.00179, PMID:35233384.
- Sun J, Li WG, Wang Q, He WP, Wang HB, Han P, *et al.* Hepatic Resection Versus Stereotactic Body Radiation Therapy Plus Transhepatic Arterial Chemoembolization for Large Hepatocellular Carcinoma: A Propensity Score Analysis. *J Clin Transl Hepatol* 2021;9(5):672–681. doi:10.14218/JCTH.2020.00188, PMID:34722182.
- Tsai CL, Hsu FM, Cheng JC. How to Improve Therapeutic Ratio in Radiotherapy of HCC. *Liver Cancer* 2016;5(3):210–220. doi:10.1159/000367767, PMID:27493896.
- Kudo M. Systemic Therapy for Hepatocellular Carcinoma: 2017 Update. *Oncology* 2017;93(Suppl 1):135–146. doi:10.1159/000481244, PMID:29258077.
- Huang CY, Lin CS, Tai WT, Hsieh CY, Shiau CW, Cheng AL, *et al.* Sorafenib enhances radiation-induced apoptosis in hepatocellular carcinoma by inhibiting STAT3. *Int J Radiat Oncol Biol Phys* 2013;86(3):456–462. doi:10.1016/j.ijrobp.2013.01.025, PMID:23474115.
- Chen SW, Lin LC, Kuo YC, Liang JA, Kuo CC, Chiou JF. Phase 2 study of combined sorafenib and radiation therapy in patients with advanced hepatocellular carcinoma. *Int J Radiat Oncol Biol Phys* 2014;88(5):1041–1047. doi:10.1016/j.ijrobp.2014.01.017, PMID:24661657.
- Page P, Yang LX. Novel chemoradiosensitizers for cancer therapy. *Anticancer Res* 2010;30(9):3675–3682. PMID:20944153.
- Voelker V, Zouhair A, Vuilleumier H, Matter M, Bouzourene H, Leyvraz S, *et al.* CPT-11 and concomitant hyperfractionated accelerated radiotherapy induce efficient local control in rectal cancer patients: results from a phase II. *Br J Cancer* 2006;95(6):710–716. doi:10.1038/sj.bjc.6603322, PMID:16940980.
- Huang G, Wang H, Yang LX. Enhancement of radiation-induced DNA damage and inhibition of its repair by a novel camptothecin analog. *Anticancer Res* 2010;30(3):937–944. PMID:20393017.
- Ghamande S, Lin CC, Cho DC, Shapiro GI, Kwak EL, Silverman MH, *et al.* A phase 1 open-label, sequential dose-escalation study investigating the safety, tolerability, and pharmacokinetics of intravenous TLC388 administered to patients with advanced solid tumors. *Invest New Drugs* 2014;32(3):445–451. doi:10.1007/s10637-013-0044-7, PMID:24271274.
- Chen AY, Chen PM, Chen YJ. DNA topoisomerase I drugs and radiotherapy for lung cancer. *J Thorac Dis* 2012;4(4):390–397. doi:10.3978/j.issn.2072-1439.2012.07.12, PMID:22934142.
- Chen BP, Chan DW, Kobayashi J, Burma S, Asaithamby A, Morotomi-Yano K, *et al.* Cell cycle dependence of DNA-dependent protein kinase phosphorylation in response to DNA double strand breaks. *J Biol Chem* 2005;280(15):14709–14715. doi:10.1074/jbc.M408827200, PMID:15677476.
- Mohiuddin IS, Kang MH. DNA-PK as an Emerging Therapeutic Target in Cancer. *Front Oncol* 2019;9:635. doi:10.3389/fonc.2019.00635, PMID:31380275.
- Nakamura N. The Role of the Transmembrane RING Finger Proteins in Cellular and Organelle Function. *Membranes (Basel)* 2011;1(4):354–393. doi:10.3390/membranes1040354, PMID:24957874.
- Ho SR, Lee YJ, Lin WC. Regulation of RNF144A E3 Ubiquitin Ligase Activity by Self-association through Its Transmembrane Domain. *J Biol Chem* 2015;290(38):23026–23038. doi:10.1074/jbc.M115.645499, PMID:26216882.
- Li HJ, Zhai NC, Song HX, Yang Y, Cui A, Li TY, *et al.* The Role of Immune Cells in Chronic HBV Infection. *J Clin Transl Hepatol* 2015;3(4):277–283. doi:10.14218/JCTH.2015.00026, PMID:26807384.
- He J, Meng M, Wang H. A Novel Prognostic Biomarker LPAR6 in Hepatocellular Carcinoma via Associating with Immune Infiltrates. *J Clin Transl Hepatol* 2022;10(1):90–103. doi:10.14218/JCTH.2021.00047, PMID:35233377.
- Weiss T, Schneider H, Silginer M, Steinle A, Pruschy M, Polić B, *et al.* NKG2D-Dependent Antitumor Effects of Chemotherapy and Radiotherapy against Glioblastoma. *Clin Cancer Res* 2018;24(4):882–895. doi:10.1158/1078-0432.CCR-17-1766, PMID:29162646.
- Bolte S, Cordelières FP. A guided tour into subcellular colocalization analysis in light microscopy. *J Microsc* 2006;224(Pt 3):213–232. doi:10.1111/j.1365-2818.2006.01706.x, PMID:17210054.
- Schüffler PJ, Fuchs TJ, Ong CS, Wild PJ, Rupp NJ, Buhmann JM. TMARKER: A free software toolkit for histopathological cell counting and staining estimation. *J Pathol Inform* 2013;4(Suppl):S2. doi:10.4103/2153-3539.109804, PMID:23766938.
- Callén E, Jančović M, Wong N, Zha S, Chen HT, Difilippantonio S, *et al.* Essential role for DNA-PKcs in DNA double-strand break repair and apo-

- ptosis in ATM-deficient lymphocytes. *Mol Cell* 2009;34(3):285–297. doi:10.1016/j.molcel.2009.04.025, PMID:19450527.
- [23] Ho SR, Mahanic CS, Lee YJ, Lin WC. RNF144A, an E3 ubiquitin ligase for DNA-PKcs, promotes apoptosis during DNA damage. *Proc Natl Acad Sci U S A* 2014;111(26):E2646–E2655. doi:10.1073/pnas.1323107111, PMID:24979766.
- [24] Lucero H, Gae D, Taccioli GE. Novel localization of the DNA-PK complex in lipid rafts: a putative role in the signal transduction pathway of the ionizing radiation response. *J Biol Chem* 2003;278(24):22136–22143. doi:10.1074/jbc.M301579200, PMID:12672807.
- [25] Hayashi M, Saito Y, Kawashima S. Calpain activation is essential for membrane fusion of erythrocytes in the presence of exogenous Ca²⁺. *Biochem Biophys Res Commun* 1992;182(2):939–946. doi:10.1016/0006-291x(92)91822-8, PMID:1734892.
- [26] Chia-Hsien Cheng J, Chuang VP, Cheng SH, Lin YM, Cheng TI, Yang PS, *et al*. Unresectable hepatocellular carcinoma treated with radiotherapy and/or chemoembolization. *Int J Cancer* 2001;96(4):243–252. doi:10.1002/ijc.1022, PMID:11474499.
- [27] Yu W, Gu K, Yu Z, Yuan D, He M, Ma N, *et al*. Sorafenib potentiates irradiation effect in hepatocellular carcinoma in vitro and in vivo. *Cancer Lett* 2013;329(1):109–117. doi:10.1016/j.canlet.2012.10.024, PMID:23142289.
- [28] Brade AM, Ng S, Brierley J, Kim J, Dinniwel R, Ringash J, *et al*. Phase I Trial of Sorafenib and Stereotactic Body Radiation Therapy for Hepatocellular Carcinoma. *Int J Radiat Oncol Biol Phys* 2016;94(3):580–587. doi:10.1016/j.ijrobp.2015.11.048, PMID:26867886.
- [29] Takeba Y, Kumai T, Matsumoto N, Nakaya S, Tsuzuki Y, Yanagida Y, *et al*. Irinotecan activates p53 with its active metabolite, resulting in human hepatocellular carcinoma apoptosis. *J Pharmacol Sci* 2007;104(3):232–242. doi:10.1254/jphs.fp0070442, PMID:17609585.
- [30] Park SH, Bang SM, Cho EK, Baek JH, Oh JH, Im SA, *et al*. First-line chemotherapy with irinotecan plus capecitabine for advanced colorectal cancer. *Oncology* 2004;66(5):353–357. doi:10.1159/000079482, PMID:15331921.
- [31] Conroy T, Paillot B, François E, Bugat R, Jacob JH, Stein U, *et al*. Irinotecan plus oxaliplatin and leucovorin-modulated fluorouracil in advanced pancreatic cancer—a Groupe Tumeurs Digestives of the Federation Nationale des Centres de Lutte Contre le Cancer study. *J Clin Oncol* 2005;23(6):1228–1236. doi:10.1200/JCO.2005.06.050, PMID:15718320.
- [32] Boige V, Taieb J, Hebbar M, Malka D, Debaere T, Hannoun L, *et al*. Irinotecan as first-line chemotherapy in patients with advanced hepatocellular carcinoma: a multicenter phase II study with dose adjustment according to baseline serum bilirubin level. *Eur J Cancer* 2006;42(4):456–459. doi:10.1016/j.ejca.2005.09.034, PMID:16427779.
- [33] Ang C, O'Reilly EM, Carvajal RD, Capanu M, Gonen M, Doyle L, *et al*. A Nonrandomized, Phase II Study of Sequential Irinotecan and Flavopiridol in Patients With Advanced Hepatocellular Carcinoma. *Gastrointest Cancer Res* 2012;5(6):185–189. PMID:23293699.
- [34] Xu L, Zhu Y, Shao J, Chen M, Yan H, Li G, *et al*. Dasatinib synergises with irinotecan to suppress hepatocellular carcinoma via inhibiting the protein synthesis of PLK1. *Br J Cancer* 2017;116(8):1027–1036. doi:10.1038/bjc.2017.55, PMID:28267710.
- [35] Cornell L, Munck JM, Alsinet C, Villanueva A, Ogle L, Willoughby CE, *et al*. DNA-PK-A candidate driver of hepatocarcinogenesis and tissue biomarker that predicts response to treatment and survival. *Clin Cancer Res* 2015;21(4):925–933. doi:10.1158/1078-0432.CCR-14-0842, PMID:25480831.
- [36] Povirk LF, Zhou T, Zhou R, Cowan MJ, Yannone SM. Processing of 3'-phosphoglycolate-terminated DNA double strand breaks by Artemis nuclease. *J Biol Chem* 2007;282(6):3547–3558. doi:10.1074/jbc.M607745200, PMID:17121861.
- [37] Ciszewski WM, Tavecchio M, Dastych J, Curtin NJ. DNA-PK inhibition by NU7441 sensitizes breast cancer cells to ionizing radiation and doxorubicin. *Breast Cancer Res Treat* 2014;143(1):47–55. doi:10.1007/s10549-013-2785-6, PMID:24292814.
- [38] Mladenov E, Iliakis G. Induction and repair of DNA double strand breaks: the increasing spectrum of non-homologous end joining pathways. *Mutat Res* 2011;711(1-2):61–72. doi:10.1016/j.mrfmmm.2011.02.005, PMID:21329706.
- [39] Ho SR, Lin WC. RNF144A sustains EGFR signaling to promote EGF-dependent cell proliferation. *J Biol Chem* 2018;293(42):16307–16323. doi:10.1074/jbc.RA118.002887, PMID:30171075.
- [40] Goodwin JF, Knudsen KE. Beyond DNA repair: DNA-PK function in cancer. *Cancer Discov* 2014;4(10):1126–1139. doi:10.1158/2159-8290.CD-14-0358, PMID:25168287.
- [41] Chen YJ, Wu H, Shen XZ. The ubiquitin-proteasome system and its potential application in hepatocellular carcinoma therapy. *Cancer Lett* 2016;379(2):245–252. doi:10.1016/j.canlet.2015.06.023, PMID:26193663.
- [42] Ciombor KK, Feng Y, Benson AB 3rd, Su Y, Horton L, Short SP, *et al*. Phase II trial of bortezomib plus doxorubicin in hepatocellular carcinoma (E6202): a trial of the Eastern Cooperative Oncology Group. *Invest New Drugs* 2014;32(5):1017–1027. doi:10.1007/s10637-014-0111-8, PMID:24890858.
- [43] Huang CY, Wei CC, Chen KC, Chen HJ, Cheng AL, Chen KF. Bortezomib enhances radiation-induced apoptosis in solid tumors by inhibiting CIP2A. *Cancer Lett* 2012;317(1):9–15. doi:10.1016/j.canlet.2011.11.005, PMID:22085493.
- [44] Jiang N, Shen Y, Fei X, Sheng K, Sun P, Qiu Y, *et al*. Valosin-containing protein regulates the proteasome-mediated degradation of DNA-PKcs in glioma cells. *Cell Death Dis* 2013;4:e647. doi:10.1038/cddis.2013.171, PMID:23722536.
- [45] Robert L, Ribas A, Hu-Lieskovan S. Combining targeted therapy with immunotherapy. *Can 1+1 equal more than 2? Semin Immunol* 2016;28(1):73–80. doi:10.1016/j.smim.2016.01.001, PMID:26861544.
- [46] Osipov A, Saung MT, Zheng L, Murphy AG. Small molecule immunomodulation: the tumor microenvironment and overcoming immune escape. *J Immunother Cancer* 2019;7(1):224. doi:10.1186/s40425-019-0667-0, PMID:31439034.
- [47] Knisely JP, Yu JB, Flanigan J, Sznol M, Kluger HM, Chiang VL. Radiosurgery for melanoma brain metastases in the ipilimumab era and the possibility of longer survival. *J Neurosurg* 2012;117(2):227–233. doi:10.3171/2012.5.JNS111929, PMID:22702482.
- [48] Rosental B, Appel MY, Yossef R, Hadad U, Brusilovsky M, Porgador A. The effect of chemotherapy/radiotherapy on cancerous pattern recognition by NK cells. *Curr Med Chem* 2012;19(12):1780–1791. doi:10.2174/092986712800099730, PMID:22414084.
- [49] Hietanen T, Pitkänen M, Kapanen M, Kellokumpu-Lehtinen PL. Effects of Single and Fractionated Irradiation on Natural Killer Cell Populations: Radiobiological Characteristics of Viability and Cytotoxicity In Vitro. *Anticancer Res* 2015;35(10):5193–5200. PMID:26408677.
- [50] Shahabi V, Postow MA, Tuck D, Wolchok JD. Immune-priming of the tumor microenvironment by radiotherapy: rationale for combination with immunotherapy to improve anticancer efficacy. *Am J Clin Oncol* 2015;38(1):90–97. doi:10.1097/COC.0b013e3182868ec8, PMID:25616204.
- [51] Wang J, Li CD, Sun L. Recent Advances in Molecular Mechanisms of the NK-G2D Pathway in Hepatocellular Carcinoma. *Biomolecules* 2020;10(2):E301. doi:10.3390/biom10020301, PMID:32075046.
- [52] Karube K, Tsuzuki S, Yoshida N, Arita K, Liu F, Kondo E, *et al*. Lineage-specific growth inhibition of NK cell lines by FOXO3 in association with Akt activation status. *Exp Hematol* 2012;40(12):1005–1015.e6. doi:10.1016/j.exphem.2012.08.005, PMID:22922206.